First published in:

ADVANCED MATERIALS

DOI: 10.1002/adma.200601497

Polarization Stop Bands in Chiral Polymeric Three-Dimensional Photonic Crystals**

By *Michael Thiel*, *Manuel Decker*, *Markus Deubel*, *Martin Wegener*, *Stefan Linden*,* and *Georg von Freymann**

Chiral 3D photonic crystals are an interesting subclass of 3D photonic crystals. For example, large complete 3D photonic bandgaps have been predicted for high-index-contrast silicon square-spiral structures;[1,2] corresponding experiments using glancing-incidence deposition,[3,4] interference lithography,[5] or direct laser writing[6,7] have been published. In addition to complete gaps or stop bands, theory[8] also predicts polarization stop bands, i.e., stop bands for just one of the two circular polarizations. Such polarization stop bands can give rise to strong circular dichroism,[4,9,10] which can potentially be used for constructing compact "thin-film" optical diodes.[11]

In this report, we fabricate high-quality polymeric 3D spiral photonic crystals via direct laser writing.[12–14] The measured transmittance spectra of these low-index-contrast structures reveal spectral regions where the transmittance is below 5 % for one circular incident polarization and above 95 % for the other—for just eight lattice constants along the propagation direction. The experimental data are compared with scattering-matrix calculations[15,16] for the actual finite structures, leading to good agreement.

For what conditions do we expect strong circular dichroism? For circular polarization of light, the tip of the electric-field vector simply follows a spiral. The pitch of this spiral is just the material wavelength λ. Thus, intuitively, we expect a chiral resonance from spiral photonic crystals if the pitch of circularly polarized light matches the pitch of the dielectric spirals, i.e., the lattice constant a_z. This condition, $\lambda/a_z = 1$, corresponds to the edge of the second Brillouin zone, i.e., to a wave number $k_z = 2\pi/\lambda = 2\pi/a_z$. Recall that the edge of the first Brillouin zone is at $k_z = \pi/a_z$. Thus, one does not anticipate a strong chiral response around and below the fundamental stop band (or bandgap), but rather at higher frequencies. Theory[8] for high-index silicon-based structures confirms this intuitive reasoning. We have repeated similar calculations for low-index-contrast polymeric structures, revealing essentially the same trends. The parameters of the 3D spiral photonic crystals to be discussed below are the result of an optimization with respect to circular dichroism.

The samples in our experiments are made by direct laser writing, which essentially allows for the fabrication of almost arbitrarily shaped 3D photoresist structures.[12–14] Details of our process based on the commercial thick-film resist SU-8 can be found in the Experimental section and in earlier work.[13] Our structures are mechanically supported by a 2D network of bars at, or close to, the top of the 3D crystal. As the spirals are not at all mechanically connected to their neighbors, very unstable low-quality structures would result without this grid. Furthermore, all the structures for optical experiments are surrounded by a thick massive wall (see Fig. 1a), which aims at reducing the effects of strain on the 2D grid caused by photoresist shrinkage during development. Here, we use a round (rather than a rectangular[13]) wall in order to evenly distribute strain inside the wall. Through numerical calculations (see below), we have confirmed that the distortion of the optical properties by the 2D network is only marginal. Most importantly, the network does not introduce any chirality.

A small gallery of selected electron microscopy images is shown in Figure 1, which gives first evidence that the sample quality is very good. Figure 1a gives an overview of the sample to be optically characterized below. The sample parameters are: in-plane lattice constant $a_{xy} = 1.3$ μm, pitch $a_z = 1.3$ μm, spiral diameter $d = 0.78$ μm, volume filling fraction 34.7 %, lateral diameter of the spiral arms $d_{\mathrm{arm}} = 380$ nm, ratio between the axial and the lateral diameter 2.7, and $N = 8$ lattice constants along the z-direction. These parameters were extracted from the close-up cross-sectional view in Figure 1a. To demonstrate the versatility of our approach, Figure 1b exhibits a cut of a structure with $a_{xy} = 1.5$ μm, $a_z = 1.5$ μm, and $N = 4$. Because the focused-ion-beam cut was stopped in between two rows of spirals, the stabilizing network mentioned

[*] Dr. S. Linden, Dr. G. von Freymann
Institut für Nanotechnologie
Forschungszentrum Karlsruhe in der Helmholtz-Gemeinschaft
76021 Karlsruhe (Germany)
E-mail: linden@int.fzk.de; freymann@int.fzk.de
Dr. S. Linden, Dr. G. von Freymann, M. Thiel, M. Decker, Dr. M. Deubel, Prof. M. Wegener
DFG-Center for Functional Nanostructures (CFN)
Universität Karlsruhe (TH)
76131 Karlsruhe (Germany)
M. Thiel, M. Decker, Dr. M. Deubel, Prof. M. Wegener
Institut für Angewandte Physik, Universität Karlsruhe (TH)
76131 Karlsruhe (Germany)

[**] We acknowledge the support provided by the Deutsche Forschungsgemeinschaft (DFG) and the State of Baden-Württemberg through the DFG-Center for Functional Nanostructures (CFN) within subproject A1.4. The research of M. W. is further supported by project DFG-We 1497/9-1, that of S. L. through a "Helmholtz-Hochschul-Nachwuchsgruppe" (VH-NG-232), and that of G. v. F. through a DFG Emmy-Noether fellowship (DFG-Fr 1671/4-3). We thank P. Brenner for assistance with the focused ion beam cutting.

© 2007 WILEY-VCH Verlag GmbH & Co. KGaA, Weinheim

EVA-STAR (Elektronisches Volltextarchiv – Scientific Articles Repository)
http://digbib.ubka.uni-karlsruhe.de/volltexte/1000010990

ADVANCED MATERIALS

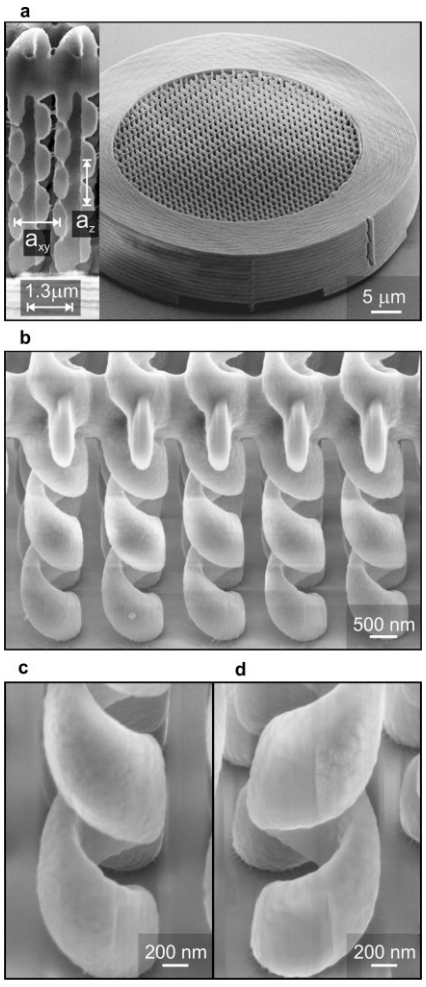

Figure 1. a–d) Gallery of fabricated 3D spiral photonic crystals. a) Oblique-incidence overview of a sample with $N = 8$ lattice constants in the z-direction, used for the measurements in Figure 2. The inset shows a close-up of a focused-ion-beam cut through the center of the spirals of an $N = 8$ structure. The inset is corrected for the oblique viewing angle. Sample parameters are $a_{xy} = a_z = 1.3$ µm and $d = 0.6a_z$. b) Close-up of the inside of a different left-handed structure with $a_{xy} = a_z = 1.5$ µm, $d = 0.6a_z$, and $N = 4$, again made accessible by focused-ion-beam cutting. c,d) Zoom-in onto one of the left-handed spirals in (b) and onto a similar, but right-handed spiral (parameters as in b), respectively.

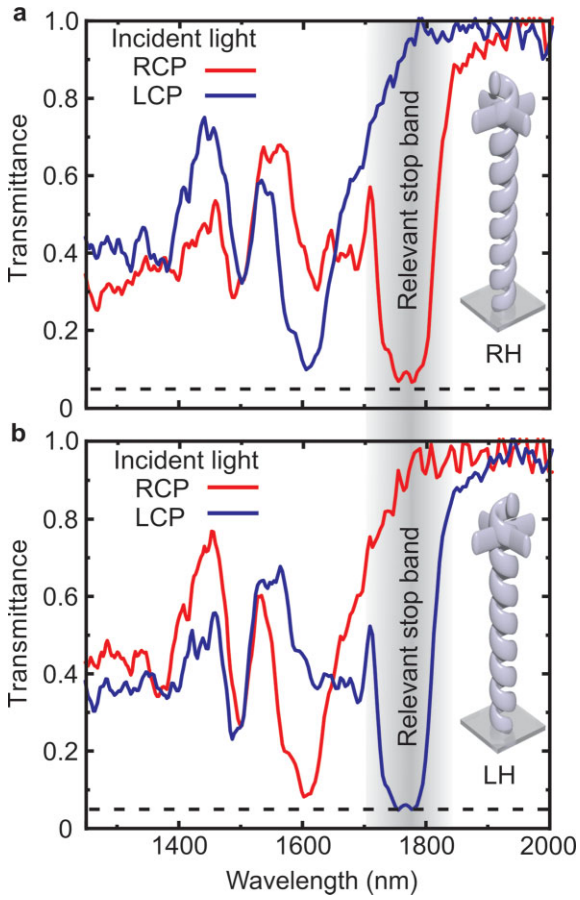

Figure 2. Measured transmittance spectra of 3D spiral photonic crystals. a) Right-handed (RH) dielectric spirals. The transmittance spectrum for right-handed circular (RCP; left-handed LCP) polarization of the incident light is shown in red (LCP: blue). The dashed horizontal lines correspond to a transmittance level of 5 %. b) Same as (a), but for left-handed (LH) dielectric spirals.

above is revealed. Figure 1c and d shows close-ups of a single left-handed spiral and a single right-handed spiral, respectively, from a sample fabricated with identical parameters but opposite handedness. We used a home-built white-light setup together with a home-built Michelson interferometer, allowing for calibrated transmittance spectroscopy on small-area samples, with small opening angles of the incident light (about 5°). The polarization state of the incident light was controlled via a Glan–Thomson polarizer and a super-achromatic quarter-wave plate. The setup gives us access to a spectral wavelength range from 500 to 2200 nm.

Figure 2 shows measured transmittance spectra of 3D circular spiral photonic crystals, with identical parameters as the ones given in Figure 1a, for both left-handed and right-handed dielectric circular spirals and for both left-handed and right-handed incident circular polarization of light. As expected from the symmetry, the transmittance spectra are nearly the same if both the sense of rotation of the dielectric spirals and that of the incident light field are changed simultaneously. At wavelengths around 1.8 µm, the transmittance in the "low state" is around 5 % compared to about 95 % in the "high state", corresponding to a ratio of ca. 20.

Figure 3 exhibits the calculated transmittance spectra corresponding to the experimental measurements (compare to Fig. 2). We employed the established scattering-matrix approach,[15,16] which can be viewed as a numerically exact solution of Maxwell's equations for the dielectric structure, which is periodic in the substrate plane but finite in the normal direction. The geometrical parameters are the same as used in the experimental measurements. In particular, we account for the ellipsoidal shape of the voxels[13] in direct laser writing. The refractive indices used for SU-8 and the glass substrate are $n_{\text{SU-8}} = 1.57$ and $n_{\text{glass}} = 1.52$, respectively. To mimic the finite opening angle of the focused incident light in the experi-

© 2007 WILEY-VCH Verlag GmbH & Co. KGaA, Weinheim

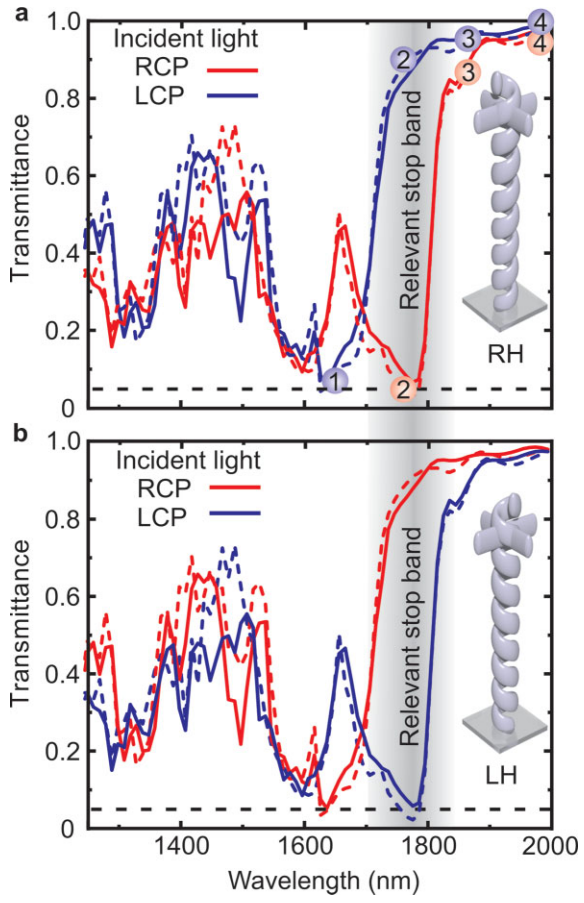

Figure 3. Calculated transmittance spectra of 3D spiral photonic crystals. Parameters and representation correspond to the experimental values (see Fig. 2). The dashed colored curves are calculations without the stabilizing grid near the top.

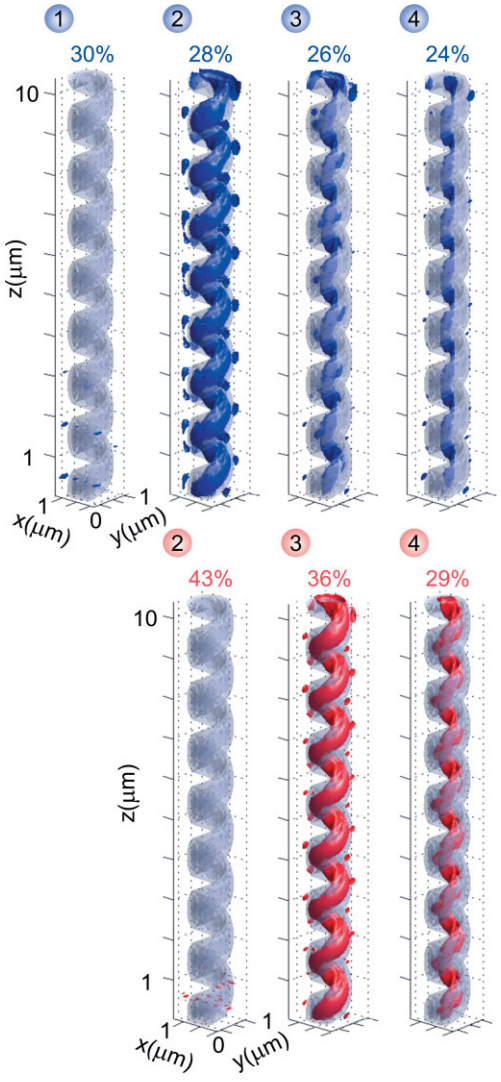

Figure 4. Illustration of the underlying physics. In each case, a right-handed dielectric spiral is depicted in gray. The colors used for the isointensity surfaces (all for 1.3 times the incident intensity of light) mark the sense of rotation of the light as in Figures 2a and 3a, i.e., red corresponds to RCP and blue to LCP. The numbers in the red and blue dots mark the spectral positions indicated in Figure 3a. The percentages quoted on the top are the fractions of the corresponding electric energy density inside the dielectric. The results for left-handed dielectric spirals are analogous with the role of LCP exchanged by RCP and vice versa (not shown).

ments, the calculated transmittance spectra are averaged over an angle of 7° with respect to the normal. It is worth noting that the overall agreement between experiment and theory is very good (Figs. 2 and 3). In particular, the symmetry, the spectral position of the polarization stop band, and the depth of the transmittance minima are reproduced very well. Quantitative deviations between experiment and theory arise at wavelengths below the polarization stop band, where many different photonic bands contribute. Moreover, one should be aware that the angle-averaging also influences the detailed shape of the spectra. For example, for the strict normal-incidence case (i.e., without any angle-averaging at all), the calculated transmittance minimum in the polarization stop band is as low as 0.1 % for the identical $N = 8$ structure.

Finally, we explain the physics underlying the polarization stop bands in spiral photonic crystals in more detail, answering the question of where the light propagates inside the structure. Figure 4 shows the underlying dielectric structure together with calculated isointensity surfaces for several relevant characteristic spectral positions (1–4, indicated in Fig. 3a) for both left-handed and right-handed circular polarization of the incident light (impinging under normal incidence with respect to the substrate). If the pitch of the light spiral inside the structure (i.e., the material wavelength) roughly matches the pitch of the dielectric spiral (i.e., the lattice constant a_z), the light field peaks inside the dielectric spiral for both senses of rotation, and no immediately obvious qualitative difference arises (compare, e.g., Fig. 4 case 1, blue with case 2, red; case 2, blue with case 3, red, etc.). Quantitatively, however, for the matching sense of rotation (red cases in Fig. 4), the confinement of the light field to the dielectric is stronger, as apparent from the fractions of the corresponding electric energy density inside the dielectric indicated above

 © 2007 WILEY-VCH Verlag GmbH & Co. KGaA, Weinheim

ADVANCED MATERIALS

the spirals in Figure 4. This effect increases the corresponding effective refractive index, hence increasing the corresponding vacuum wavelength of the polarization stop band. Clearly, within the polarization stop band, the light intensity decays exponentially along the propagation direction (case 1, blue and case 2, red in Fig. 4). Consequently, one gets a polarization stop band for each of the two circular polarizations (see Fig. 3). Obviously, the short-wavelength polarization stop band is not attractive for practical applications because the transmittance in the opposite circular polarization does not come close to unity.

In conclusion, we have observed polarization stop bands connected with strong circular dichroism from artificial and tailored chiral dielectric photonic crystals. This progress has become possible by employing very high-quality 3D polymeric structures fabricated via direct laser writing. In the future, heterostructures of such chiral structures could be applied as inexpensive and compact "thin-film" optical diodes—without the need for static magnetic fields used in commercial Faraday isolators. Importantly, we have shown that only a few lattice constants of low-index-contrast polymeric structures can already provide very large effects. In the case of, for example, $N = 8$ periods, the high-transmittance value is above 95 %, the theoretical ideal (i.e., normal incidence) low-transmittance value is below 0.1 %. For comparison, commercially available Faraday isolators have best high-transmittance values of around 90 % and best low-transmittance values of 0.01 % (typical 0.1–0.05 %). Increasing the number of periods beyond $N = 8$ clearly improves the performance in principle, but is currently not possible due to technical limitations. These limitations might be overcome following recent suggestions.[17] The effects would, however, be even larger if the polymer structure was replicated via the recently introduced silicon double-inversion procedure.[18]

Experimental

We employed 3 mW of average power derived from an 82 MHz repetition frequency sub-100 fs pulse-duration-mode locked laser oscillator at 800 nm center wavelength (Spectra-Physics Tsunami).

The structure was programmed with a 100 nm point spacing, which gave a smooth surface of the spirals. With an update rate of 100 points per second, the whole structure was fabricated in ca. 45 min. The high repetition rate of the laser system ensured a smooth distribution of the effective dose during the writing of the trajectories connecting these points. This is consistent with earlier overall findings [17], although the authors used an amplified system. On the basis of woodpile structures [13], we have not found any significant differences in the optical quality of structures written with a low repetition rate amplified system and with a high repetition rate oscillator. Thermal effects, as addressed in previous work [17], were not relevant under these conditions. The oscillator system is obviously less expensive. Moreover, it potentially allows for higher writing speeds and, hence, for reduced processing times. All details on the treatment of the photoresist have been reported earlier [13]. In particular, we did use a post-bake step—in contrast to experimental details published earlier [17].

Received: July 5, 2006
Revised: August 15, 2006
Published online: January 3, 2007

[1] A. Chutinan, S. Noda, *Phys. Rev. B: Condens. Matter Mater. Phys.* **1998**, *57*, 2006.
[2] O. Toader, S. John, *Science* **2001**, *292*, 1133.
[3] S. R. Kennedy, M. J. Brett, O. Toader, S. John, *Nano Lett.* **2002**, *2*, 59.
[4] P. C. P. Hrudey, B. Szeto, M. J. Brett, *Appl. Phys. Lett.* **2006**, *88*, 251 106.
[5] Y. K. Pang, J. Lee, H. Lee, W. Y. Tam, C. Chan, P. Sheng, *Opt. Express* **2005**, *13*, 7615.
[6] K. K. Seet, V. Mizeikis, S. Matsuo, S. Juodkazis, H. Misawa, *Adv. Mater.* **2005**, *17*, 541.
[7] K. K. Seet, V. Mizeikis, S. Juodkazis, H. Misawa, *Appl. Phys. A* **2006**, *82*, 683.
[8] J. Lee, C. Chan, *Opt. Express* **2005**, *13*, 8083.
[9] S. Furumi, Y. Sakka, *Adv. Mater.* **2006**, *18*, 775.
[10] M. Mitov, N. Dessaud, *Nat. Mater.* **2006**, *5*, 361.
[11] J. Hwang, M. H. Song, B. Park, S. Nishimura, T. Toyooka, J. W. Wu, Y. Takanishi, K. Ishikawa, H. Takezoe, *Nat. Mater.* **2005**, *4*, 383.
[12] S. Kawata, H.-B. Sun, T. Tanaka, K. Takada, *Nature* **2001**, *412*, 697.
[13] M. Deubel, G. von Freymann, M. Wegener, S. Pereira, K. Busch, C. M. Soukoulis, *Nat. Mater.* **2004**, *3*, 444.
[14] M. Deubel, M. Wegener, S. Linden, G. von Freymann, S. John, *Opt. Lett.* **2006**, *31*, 805.
[15] D. M. Whittaker, I. S. Culshaw, *Phys. Rev. B: Condens. Matter Mater. Phys.* **1999**, *60*, 2610.
[16] S. G. Tikhodeev, A. L. Yablonskii, E. A. Muljarov, N. A. Gippius, T. Ishihara, *Phys. Rev. B: Condens. Matter Mater. Phys.* **2002**, *66*, 045 102.
[17] K. K. Seet, S. Juodkazis, V. Jarutis, H. Misawa, *Appl. Phys. Lett.* **2006**, *89*, 024 106.
[18] N. Tétreault, G. von Freymann, M. Deubel, M. Hermatschweiler, F. Pérez-Willard, S. John, M. Wegener, G. A. Ozin, *Adv. Mater.* **2006**, *18*, 457.

 © 2007 WILEY-VCH Verlag GmbH & Co. KGaA, Weinheim